Molecular Vision 2021; 27:78-94 <http://www.molvis.org/molvis/v27/78>
Received 1 May 2020 | Accepted 3 February 2021 | Published 5 February 2021

Clinical and genetic findings in Italian patients with sector retinitis pigmentosa

Tommaso Verdina,[1] Vivienne C. Greenstein,[2] Stephen H. Tsang,[3,4] Vittoria Murro,[5] Dario Pasquale Mucciolo,[5] Ilaria Passerini,[6] Rodolfo Mastropasqua,[1] Gian Maria Cavallini,[1] Gianni Virgili,[5] Fabrizio Giansanti,[5] Andrea Sodi[5]

[1]Institute of Ophthalmology, University of Modena and Reggio Emilia, Modena, Italy; [2]Department of Ophthalmology, Columbia University, New York, NY; [3]Jonas Children's Vision Care, and Bernard & Shirlee Brown Glaucoma Laboratory, Columbia Stem Cell Initiative, Departments of Ophthalmology, Pathology & Cell Biology, Institute of Human Nutrition, Vagelos College of Physicians and Surgeons, Columbia University, New York, NY; [4]Edward S. Harkness Eye Institute, New York-Presbyterian Hospital, New York, NY; [5]Department of Neuroscience, Psychology, Drug Research and Child Health, University of Florence, Florence, Italy; [6]Department of Genetic Diagnosis, Careggi Teaching Hospital, Florence, Italy

Purpose: To describe clinical and genetic features in a series of Italian patients with sector retinitis pigmentosa (sector RP).

Methods: Fifteen patients with sector RP were selected from the database of Hereditary Retinal Degenerations Referring Center of Careggi Hospital (Florence, Italy). Eleven patients from five independent pedigrees underwent genetic analysis with next-generation sequencing (NGS) confirmed with Sanger sequencing. The diagnosis of sector RP was based on the detection of topographically limited retinal abnormalities consistent with corresponding sectorial visual field defects. Best-corrected visual acuity (BCVA), fundus color pictures as well as fundus autofluorescence (FAF), spectral domain-optical coherence tomography (SD-OCT), full-field electroretinography (ERG), and 30–2 Humphrey visual field (VF) data were retrospectively collected and analyzed.

Results: For the 30 eyes, the mean BCVA was 0.05 ± 0.13 logMAR, and the mean refractive error was −0.52 ± 1.89 D. The inferior retina was the most affected sector (86.7%), and the VF defect corresponded to the affected sector. FAF showed a demarcation line of increased autofluorescence between the healthy and affected retina, corresponding on SD-OCT to an interruption of the ellipsoid zone (EZ) band in the diseased retina. Dark-adapted ERG amplitudes were decreased in comparison to normative values. In five unrelated families, the sector RP phenotype was associated with sequence variants in the *RHO* gene. The same mutation c.568G>A p.(Asp190Asn) was found in nine patients of four families.

Conclusions: Typical sector RP is a mild form of RP characterized by preserved visual acuity with limited retinal involvement and, generally, a more favorable prognosis than other forms of RP.

Retinitis pigmentosa (RP) is a group of inherited retinal disorders characterized by photoreceptor degeneration, progressive peripheral visual field loss, and night blindness. Sector RP is an atypical form of RP first described by Bietti in 1937 [1] characterized by retinal degeneration with bone spicule-like pigmentation limited to a retinal quadrant (typically the lower nasal) usually with bilateral symmetric involvement [2]. The typical forms, generally diagnosed in midlife, are usually associated with a more favorable prognosis [3]. However, RP has been reported to occur sometimes in pedigrees where other family members have typical/classic or diffuse RP [4].

Correspondence to: Tommaso Verdina, Struttura Complessa di Oftalmologia, Azienda Ospedaliero-Universitaria di Modena Policlinico, Via del Pozzo 71, 41100, Modena, Italy; Phone: 0039 059 360309; FAX: 0039 059 371532; email: tommaso.verdina@gmail.com

There are a limited number of reports of patients with sector RP in the literature, and the natural history of this condition and its phenotypic variability are still unclear and remain to be determined. In particular, it is still debated whether sector RP is a stationary or slowly progressive disease [5,6]. Autosomal dominant sector RP has been associated with pathogenic mutations in the *rhodopsin* (*RHO*; Gene ID: 6010, OMIM 180380) gene in various ethnic populations [7-14], while mutations in other genes have been detected in autosomal recessive [15-18] and X-linked forms [9,19]. We report for the first time on the clinical and genetic features of a relatively large series of Italian patients diagnosed with sector RP.

METHODS

In this retrospective study, patients with a clinical diagnosis of sector RP were selected from the database of the Hereditary Retinal Degenerations Referring Center of Careggi Teaching

Hospital in Florence (Italy). The medical records and results of imaging studies of 30 eyes of 15 consecutive patients were retrospectively reviewed according to the guidelines of the local Ethical Committee at the Florence Careggi teaching Hospital. All procedures were reviewed and deemed to be in accordance with the tenets of the Declaration of Helsinki for research involving human participants.

The criteria for inclusion was based on the presence of characteristic sector RP fundus features, that is, bone spicule-like pigmentation in one or two retinal quadrants with sparing of the other quadrants and associated VF defects corresponding to the altered retina. We included primarily patients with known pathogenic mutations associated with RP. Patients with unknown genotypes were considered only if their clinical picture agreed with the clinical inclusion criteria above.

Patients were excluded from the study if they had other ocular diseases or systemic disorders that could affect the results of the multimodal and visual function tests (except related retinal alterations) or cataract with nuclear sclerosis grade ≥2 (NS2) in the Lens Opacities Classification System III (LOCS III) [20]. All patients underwent a complete ophthalmic examination with evaluation of best-corrected visual acuity (BCVA), autorefractometry (Autorefractometer AR-600; Nidek, Padova, Italy), and biomicroscopy of anterior and posterior chambers. Ocular mydriasis was obtained with Visumidriatic Tropicamide 1% ® drops (Visufarma Srl, Rome, Italy). Fundus imaging was performed using a Zeiss retinograph with image processing software VISUPAC (Carl Zeiss, Dublin, CA) to document the localization of bone spicule-like pigmentation.

Fundus autofluorescence (FAF) imaging was performed with a confocal scanning laser ophthalmoscope (Heidelberg Retina Angiograph 2 or Spectralis HRA+OCT; Heidelberg Engineering, Dossenheim, Germany) using a 30° field of view at a resolution of 1,536 × 1,536 pixels. An optically pumped solid-state laser (488 nm) was used for excitation, and a 495 nm barrier filter was used to modulate the blue argon excitation light. Standard procedure was followed for the acquisition of FAF images, including focus of the retinal image in the infrared reflection mode at 820 nm, sensitivity adjustment at 488 nm, and acquisition of nine single 30° × 30° images. The nine single images were computationally averaged to produce a single frame with improved signal-to-noise ratio. In particular, we identified three FAF patterns: normal (N-AF), hyper-autofluorescence (hyper-AF), and hypoautofluorescence (hypo-AF).

Spectral domain-optical coherence tomography (SD-OCT) was performed in all patients in the macular area and in the area with bone spicule-like pigmentation. Spectralis HRA+OCT was used for 11 patients and Zeiss Cirrus OCT 4000 (Carl Zeiss) for four patients. Both instruments allow for simultaneous OCT scans and fundus photography and subsequent image superimposition. The acquisition protocol consisted of a macular cube 512 × 128 scan pattern in which a 6.0 × 6.0 mm region of the retina was scanned (a total of 65.536 sampled points) within a scan time of 2.4 s and a raster vertical line which passed simultaneously through the pigmented area and the fovea. The precise location and orientation of each scan were determined using the simultaneous OCT grayscale fundus images. The ellipsoid zone (EZ) band was identified on the OCT scans and classified as present (well-defined), disrupted (poorly defined or disorganized), or absent (complete absence of the EZ band). Macular edema was defined as a central foveal thickness greater than 250 µm with intraretinal hyporeflectivity cysts. Each OCT scan was independently evaluated by three different observers (TV, VM, and AS). In cases of disagreement between the observers, the opinion of the senior observer (AS) was considered.

Visual fields (VFs) were obtained using a Humphrey perimeter (Carl Zeiss Meditec Inc., Oberkirchen, Germany), the 30–2 pattern, and the Swedish Interactive Threshold Algorithm (SITA)-standard protocol. Electroretinography (ERG) was performed using the International Society for Clinical Electrophysiology of Vision (ISCEV) standard protocol [21]. Following pupil dilation, ERGs were obtained using Retiscan 201 B4 (Roland Consult, Brandenburg, Germany). Dark-adapted full-field ERGs were recorded following stimulation with white flashes of intensities of 0.01 and 3.0 cd.s.m^2. Photopic cone system function was assessed after 10 min of light adaptation by recording ERGs to 3.0 cd.s.m^2. We compared the results with those obtained from a group of age-similar control patients (n = 15) with no significant ocular pathology who attended our clinic. An Excel database (Microsoft Excel 2010, Microsoft Office Professional Plus 2010) was used to record all the data. The data were analysed by means of Stata 13.1 software (StataCorp LP, College Station, TX), using the Student's t-test with statistical significance set at a p-value <0.05.

Following informed consent and a complete medical history of each patient, 10 ml of peripheral blood were obtained from the antecubital vein using EDTA-containing vials. DNA was extracted from 200 µl of peripheral blood by using automated DNA extractors: BioRobot EZ1 (QIAGEN, Hilden, Germany) or QIAsymphony SP workstation (QIAGEN GmbH, Germany), according to the manufacturer protocols. The mode of inheritance was analyzed in all

patients; in each family, the proband was the first patient with a clinical diagnosis of RP included in the study. In 11 probands from five independent pedigrees, genetic analysis was performed with targeted next-generation sequencing (NGS) at the Department of Genetic Diagnosis (Careggi Teaching Hospital, Florence, Italy) which is a certified UNI EN ISO 9001:2008 laboratory. A panel of 137 genes known to be associated with retinal dystrophies was used for targeted NGS: Exons of DNA samples were captured and investigated as shown previously with enrichment methodology SureSelect QXT Target Enrichment (Agilent Technologies, Santa Clara, CA), using the Illumina NextSeq TM500 platform (Illumina, San Diego, CA). All identified variants were confirmed with Sanger sequencing and further segregated in the respective families when other relatives were available. Variants' pathogenicity was evaluated with InterVar, a bioinformatic software tool for clinical interpretation of genetic variants according to the classification proposed by the America College of Medical Genetics and Genomics [22].

RESULTS

Thirty eyes of 15 patients (six men and nine women) from nine independent pedigrees were included in the study. The average (± standard deviation) age was 50.14 ± 18.20 years (range 19–77 years). Mean age at onset was 41.20 ± 15.51 years (range 11–69 years). Pathogenic mutations were identified in nine patients; two patients carried variants of uncertain significance (VUS), and four patients were not available for genetic testing. Selected demographic, clinical, and genetic features of the study population are summarized in Table 1.

Visual acuity and refraction: The mean BCVA was 0.05 ± 0.13 logMAR (range 0–0.52 logMAR; 20/20–20/66 Snellen acuity), and the mean refractive error was −0.52 ± 1.89 D spherical equivalent (range −6.50 to +3.00 D, see Table 1). Five out of 30 eyes presented with a low-grade NS1 cataract, one eye was pseudophakic without any surgery-related complication, and 25 eyes had no evidence of cataract.

Fundus evaluation and retinography: In all patients, bone spicule-like pigmentation was observed in the affected sectors of the retina. On ophthalmoscopy, two patients showed bilateral vitreomacular adhesions (vitreoretinal interface syndrome). There was no evidence of abnormal and irregular retinal appearance in the macular region in any of the 30 eyes. All patients, except one (P12), presented with symmetric alterations of the pigmented area in both eyes. For 14 patients (28 eyes), the inferior hemiretina was the most affected area (see the examples in Figure 1A,B); for three of the 14 (P1, P4, P11) the nasal quadrant was also affected, and for two (P6, P10), the temporal quadrant. In one patient (P7), the pigmented area had a diffuse appearance with involvement of the superior sector, whereas for another patient (P12), the pigmented area was nasal in the right eye and temporal in the left eye. No patient showed alterations in the superior retina (see Table 1).

Visual field: For all eyes, the VF defects corresponded to the retinal areas of degeneration. Figure 2 provides an example of correspondence between superior VF defects and inferior retinal changes for P13. Figure 3 illustrates the correspondence between the superior VF defect and FAF changes in the inferior retina for P1; the hyper-AF arc reflects the transition between "normal" and "abnormal" retinal function.

Fundus autofluorescence: In all patients, except P15, we found a band of markedly hyper-AF which was associated with the transition zone between the normal-functioning retina and the diseased retina, and corresponded to the scotomatous area on the VF (Figure 4, Figure 5, and Figure 6). This demarcation band does not match the border of the pigmented RPE areas as seen on retinography and FAF, but it appears to be localized nearer to the posterior pole. Figure 7 shows wide-angle retinography and FAF in P15 without the hyper-AF band and with the area of pigmentary changes located more peripherally.

Optical coherence tomography: On OCT, there was no evidence of macular edema in the 30 eyes. We observed epiretinal membranes in four eyes. Interestingly, the OCT performed in the area with the hyper-FAF line showed the presence of the EZ band in the relatively "healthy" retina nearer to the posterior pole, absence of the EZ band with the presence of RPE in the transition zone, and absence of the EZ and RPE in the severely affected retina. Two typical examples are shown in Figure 8A,B: The yellow line indicates the OCT scan line and the blue line the intact EZ band. The two arrows indicate the internal (the outer border of hyper-AF band) and external boundaries (adjacent to atrophic RPE with bone spicule-like pigmentation), respectively, of the transition zone. We also obtained horizontal OCT line scans in the region of the bone spicules, and we noticed that bone spicules are localized within the retinal layers (in particular at the level of the outer plexiform layer) with an underlying choroid with prominent enlarged choroidal vessels (Figure 9).

Electrophysiology: No delays in implicit times were observed. All patients had decreased scotopic ERG response amplitudes compared to the healthy controls; the photopic response amplitudes were within normal limits. The results are summarized in Table 2.

Genetic analysis: Nine patients of three independent pedigrees showed a clear dominant inheritance (two from family

Table 1. Demographic, clinical and genetic data of the study population.

ID	Age	Sex	Eye	Onset	BCVA logMar	Snellen	sph eq.	Affected sector	GENE/cDNA(protein)
P1 (AG)*	69	F	R	40	0	20/20	0	INF, NAS	RHO /c.568G>A(p.Asp190Asn)
			L		0	20/20	0	INF, NAS	
P2 (AM)*	65	M	R	36	0	20/20	-2	INF	RHO /c.568G>A(p.Asp190Asn)
			L		0	20/20	-2	INF	
P3 (BA)	53	F	R	46	0.1	20/25	-2.5	INF	
			L		0.3	20/40	-3.5	INF	
P4 (FO)	77	F	R	69	0.52	20/60	3.5	INF, NAS	
			L		0.1	20/25	0.75	INF, NAS	
P5 (FA)	57	M	R	44	0	20/20	0	INF	RHO/c.568G>A(p.Asp190Asn)
			L		0	20/20	0	INF	
P6 (GL)	64	M	R	62	0	20/20	0	INF, TEMP	RHO /c.568G>A(p.Asp190Asn)
			L		0	20/20	-1.25	INF, TEMP	
P7 (PP)	58	F	R	50	0	20/20	2	INF,TEMP,NAS	
			L		0	20/20	2.25	INF,TEMP,NAS	
P8 (RM)	40	F	R	40	0	20/20	0	INF	RHO /c.548T>C (p.Leu183Pro)
			L		0	20/20	0	INF	
P9 (SA)**	63	M	R	52	0	20/20	0.5	INF	RHO /c.568G>A (p.Asp190Asn)
			L		0	20/20	0.5	INF	
P10 (SE)**	19	F	R	11	0	20/20	0.75	INF, TEMP	
			L		0	20/20	0.25	INF, TEMP	
P11 (SF)**	23	F	R	21	0	20/20	-0.75	INF, NAS	RHO /c.568G>A (p.Asp190Asn)
			L		0	20/20	-0.5	INF, NAS	
P12 (SL)**	22	F	R	21	0	20/20	0	NAS	RHO /c.568G>A (p.Asp190Asn)
			L		0	20/20	0	TEMP	
P13(SM)**	57	M	R	48	0	20/20	0	INF	RHO /c.568G>A (p.Asp190Asn)
			L		0	20/20	0	INF	
P14 (SS)**	29	F	R	28	0	20/20	-2	INF	RHO /c.568G>A (p.Asp190Asn)
			L		0	20/20	-2	INF	GUCY2D /c.2179G>A (p.Gly727Ser)
P15 (TA)	56	M	R	50	0.4	20/50	-8	INF	USH2A/c.2173G>C(p.Gly713Arg); ROM1 /c.178C>A (p.Pro60Thr)c.323C>T (p.Thr108Met)

BCVA in logMar and Snellen equivalent. Sph eq.=spherical equivalent; R=right eye; L=left eye; INF: inferior; SUP: superior; NAS: nasal ; TEMP: temporal. *family A; ** family S

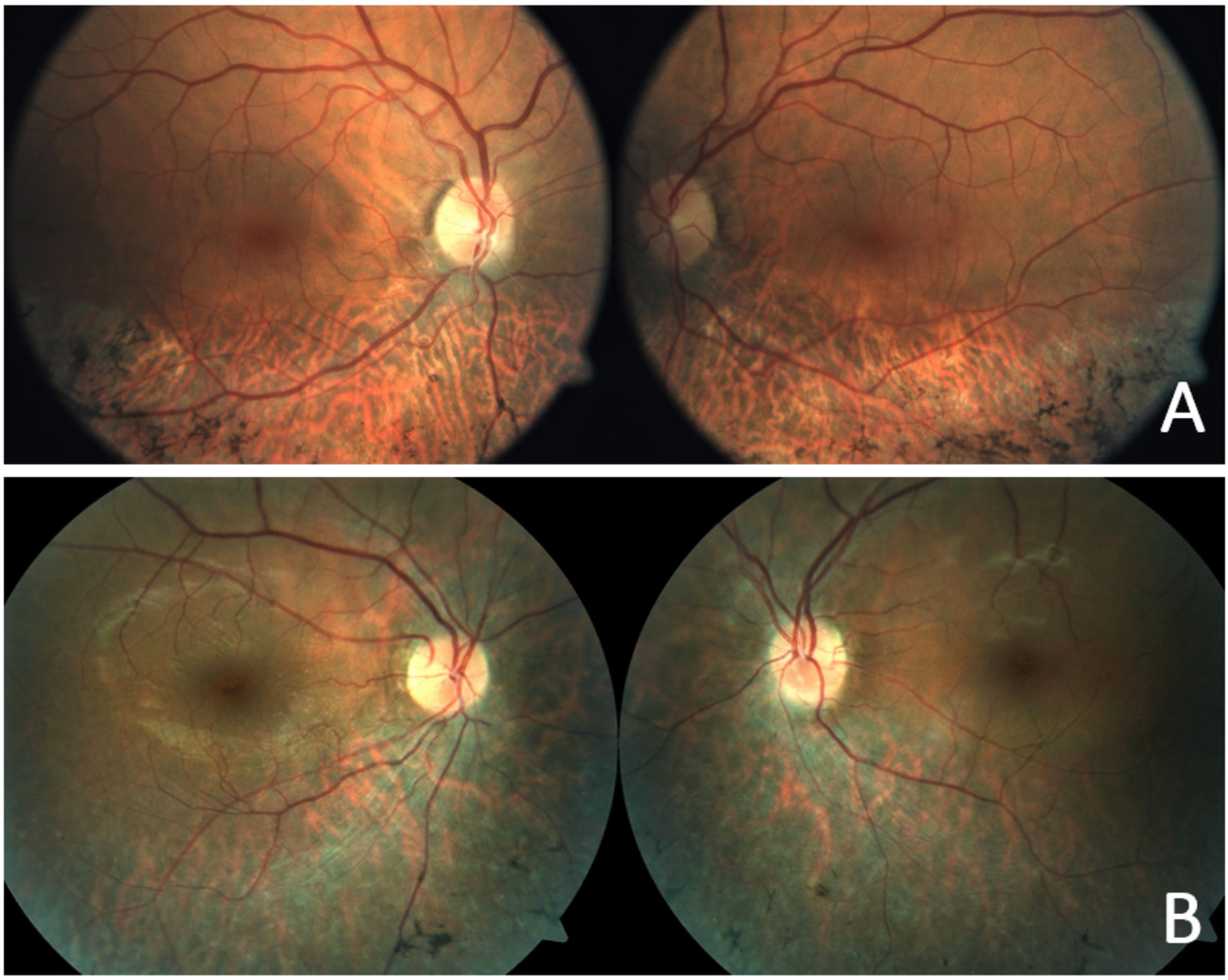

Figure 1. Color retinography imaging. Bone spicule-like pigmentation in the inferior retina with symmetric alterations of the pigmented area in both eyes in patient 5 (**A**) and patient 11 (**B**).

A, six from family S, and one from family T). The other patients appeared with sporadic forms, but in those cases, we could not examine the remaining family members. The pedigrees of families A, S, and T are reported in Figure 10.

In 11 patients from five independent pedigrees, blood samples were obtained for genetic analysis. The same mutation c.568G>A p.(Asp190Asn) in the gene encoding *RHO* (Online Mendelian Inheritance in Man (OMIM), 180,380) was found in nine patients of four different families. This variant has been reported [23-29] in association with RP and can be considered pathogenic. Another patient (P8) from an independent pedigree carried a novel variant c.548T>C (p.Leu183Pro) in the same *RHO* gene. This variant was interpreted as a VUS by the predictive software InterVar. All patients carrying the mutations in *RHO* had clinical manifestations of sector RP. An "additional" variant of the *GUCY2D* gene (OMIM, 600,179; c.2179G>A (p.Gly727Ser) was found in one patient (P14) in heterozygous state. As this variant has been reported as non-disease-causing [30], and it is present only in one patient whose phenotype is fully explained by a surely pathogenic *RHO* variant, the patient can be considered a heterozygous carrier of a VUS that likely does not contribute to the patient's disease. The last patient (P15) who underwent genetic analysis carried two in "*cis*" variants of the *ROM1* gene (OMIM, 180,721), (c.178C>A (p.Pro60Thr) and c.323C>T (p.Thr108Met). This genotype has been reported in association with the RP phenotype, but its pathogenicity is uncertain, and they are considered VUS

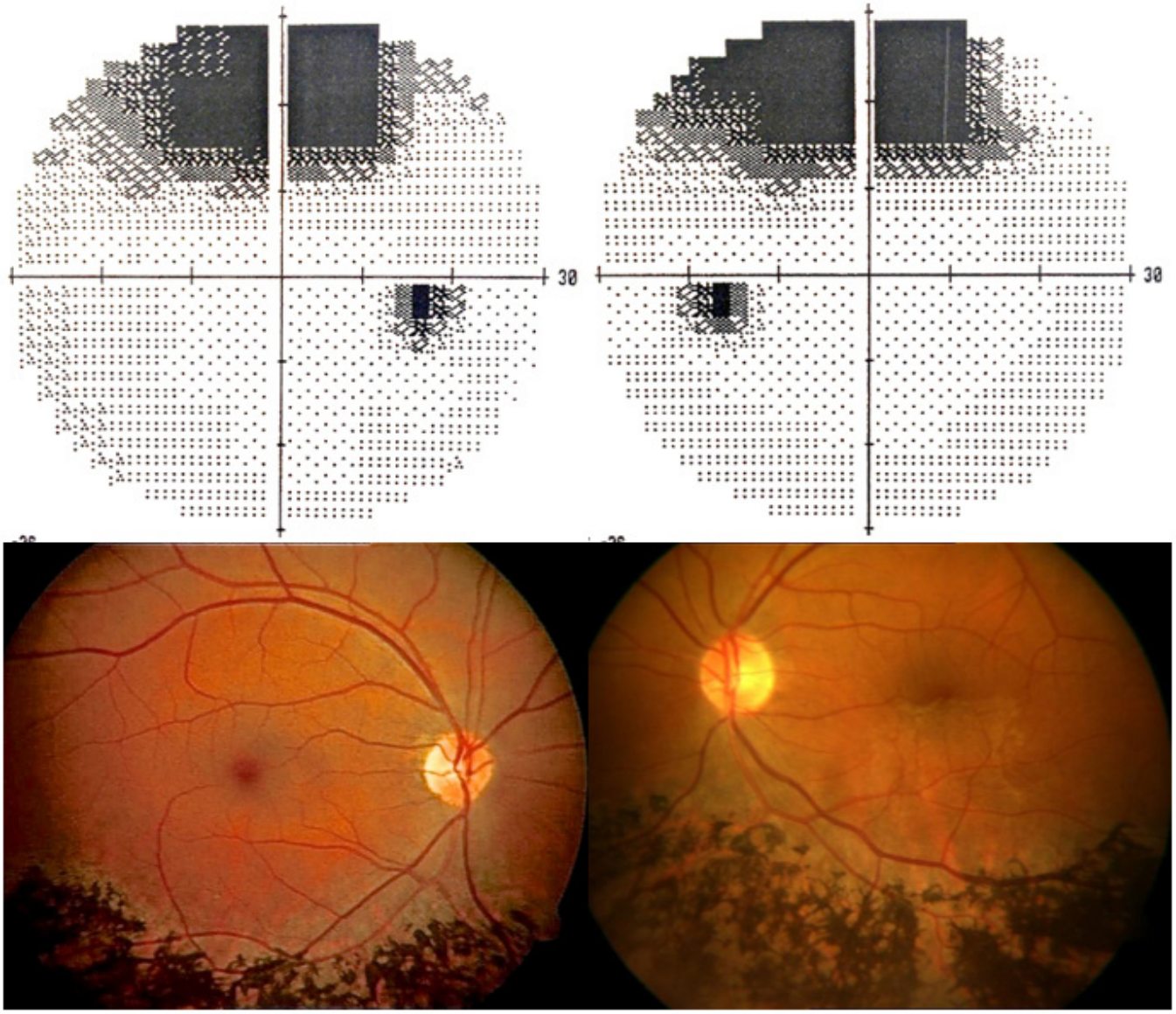

Figure 2. 30–2 visual field testing and corresponding color retinography in both eyes in patient 13. The visual field shows superior scotomatous defect while retinography shows the corresponding inferior retinal degeneration with bone spicules pigmentation.

[31-33]. The remaining four patients (P3, P4, P7, and P10 from family S) were not available for molecular study.

DISCUSSION

In this study, we describe the phenotype and genetic features of a group of Italian patients affected by a typical form of sector RP. In this cohort, we found relatively good BCVA in agreement with previous studies [7-9], and with reports of a benign clinical natural history in which patients usually maintain good visual acuity and become aware of the disease after a long time [34-38]. One exception in the literature was the report of a patient in a study by Coussa et al. [9] who showed a significant reduction in bilateral visual acuity. Another finding of interest was that only five eyes out of 30 presented with a low-grade cataract, and one underwent cataract surgery; this percentage was lower than that reported for classic RP (more than 50%) [39]. This result could be due to the limited number of patients in this study or to their relatively young age; however, it is possible that this is another example of milder ocular complications in sector RP.

In agreement with previous findings, the most commonly affected retinal area was the inferior retina [7-9,34-37]. This has been explained based on preferential exposure of the inferior retina to the light coming from typically overhead

Figure 3. Color retinography, fundus autofluorescence, and visual field testing for left eye in patient 1. The image shows the correspondence between the inferior retinal degeneration and the superior hemifield defect.

light sources (i.e., sunlight and indoor illumination) [40,41]. The bilateral and symmetric topographic involvement of the pigmentary alterations in accordance with the genetic cause of the disease has also been reported [7-9,34].

On FAF, we found a demarcation line of hyper-AF in the affected quadrant. In RP, the hyperfluorescent ring is considered to represent the boundary between functional and non-functional areas of the retina. Specifically, the edge of the ring corresponds to the internal border of the visual field defect [37]. Popovic et al. [42] noted a good correlation between the radius of the hyper-AF ring and visual field sensitivity; the authors concluded that the healthy retina was located within the ring, and the diseased retina was peripheral to the hyper-AF ring. In agreement with these findings in patients with sector RP, Fleckenstein et al. [43] and Lima et al. [44] described an interruption of the EZ band and a decrease in the outer nuclear layer thickness straddling the perimeter of the hyper-AF ring. Wakabayashi [45] observed that the hyper-AF ring could represent the regional distribution of the active degeneration of the photoreceptors, i.e., a region with a high rate of phagocytosis of the photoreceptors' outer segments by the RPE. When the accumulation of lipofuscin has reached a critical level, this induces the signal captured by the FAF at its maximum intensity. RPE cells die with

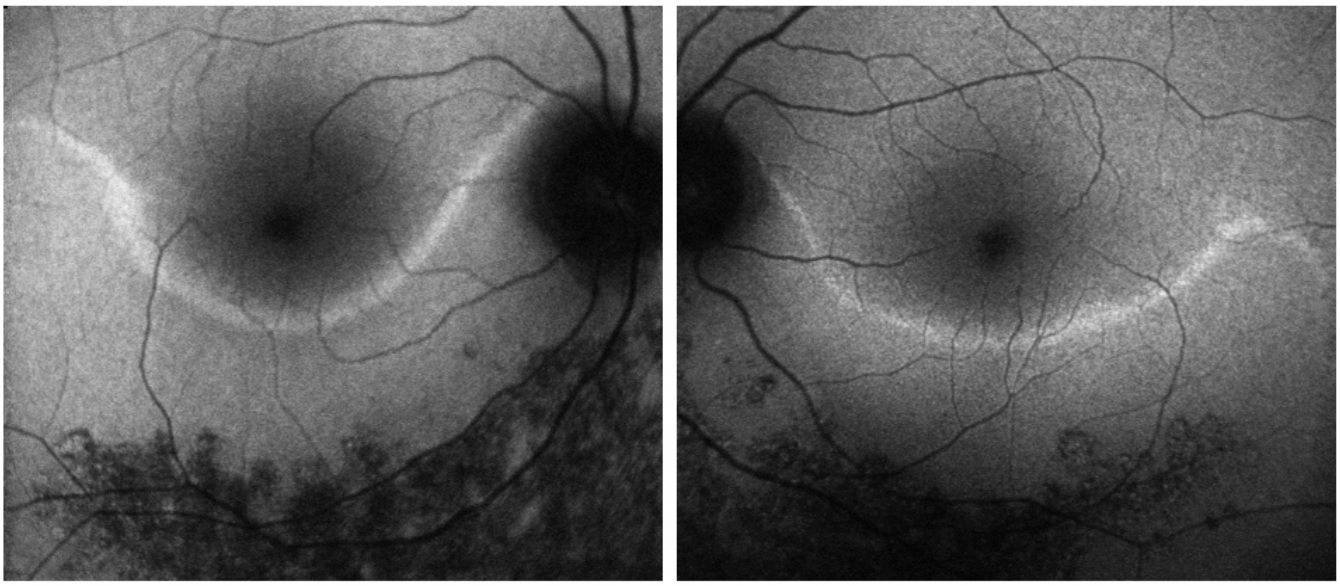

Figure 4. Fundus autofluorescence imaging. The images are related to patient 3 and show hyper-AF arcs associated with the transition zone between the normal-functioning retina and the diseased retina.

a concomitant loss of lipofuscin granules. Photoreceptor death leads to RPE atrophy and the consequent absence of detectable fluorescence [46] that can be seen in the retinal periphery. Duncker et al. [47] described a case of sector RP with a continuous line of higher autofluorescence outlining the affected retina suggesting that this band could originate from dying photoreceptor cells.

In the analysis, we noted that in sector RP the line of hyper-AF corresponded to the interruption of the EZ band on OCT (Figure 8). The peripheral dark area on FAF appeared to be far from the hyper-AF band with the presence of a transitional area between the two. In this transitional area, the retina was thinner; on OCT, the EZ band was absent, the RPE was present, and FAF appeared to be normal. This transitional

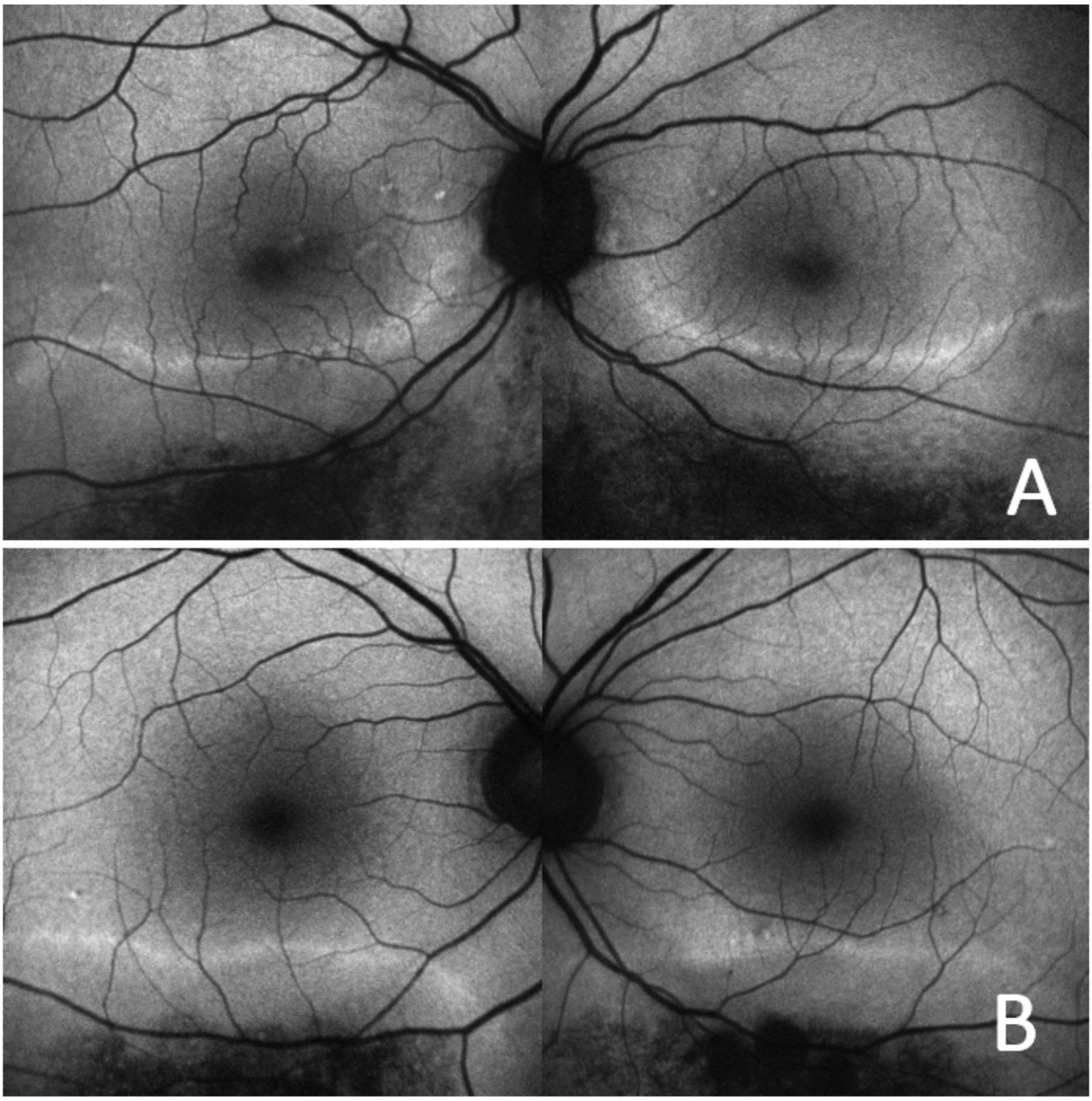

Figure 5. Fundus autofluorescence imaging. The images show the demarcation line of hyper-AF in the affected quadrant in patient 1 (**A**) and patient 2 (**B**). This line represents the boundary between functional and non-functional areas of the retina.

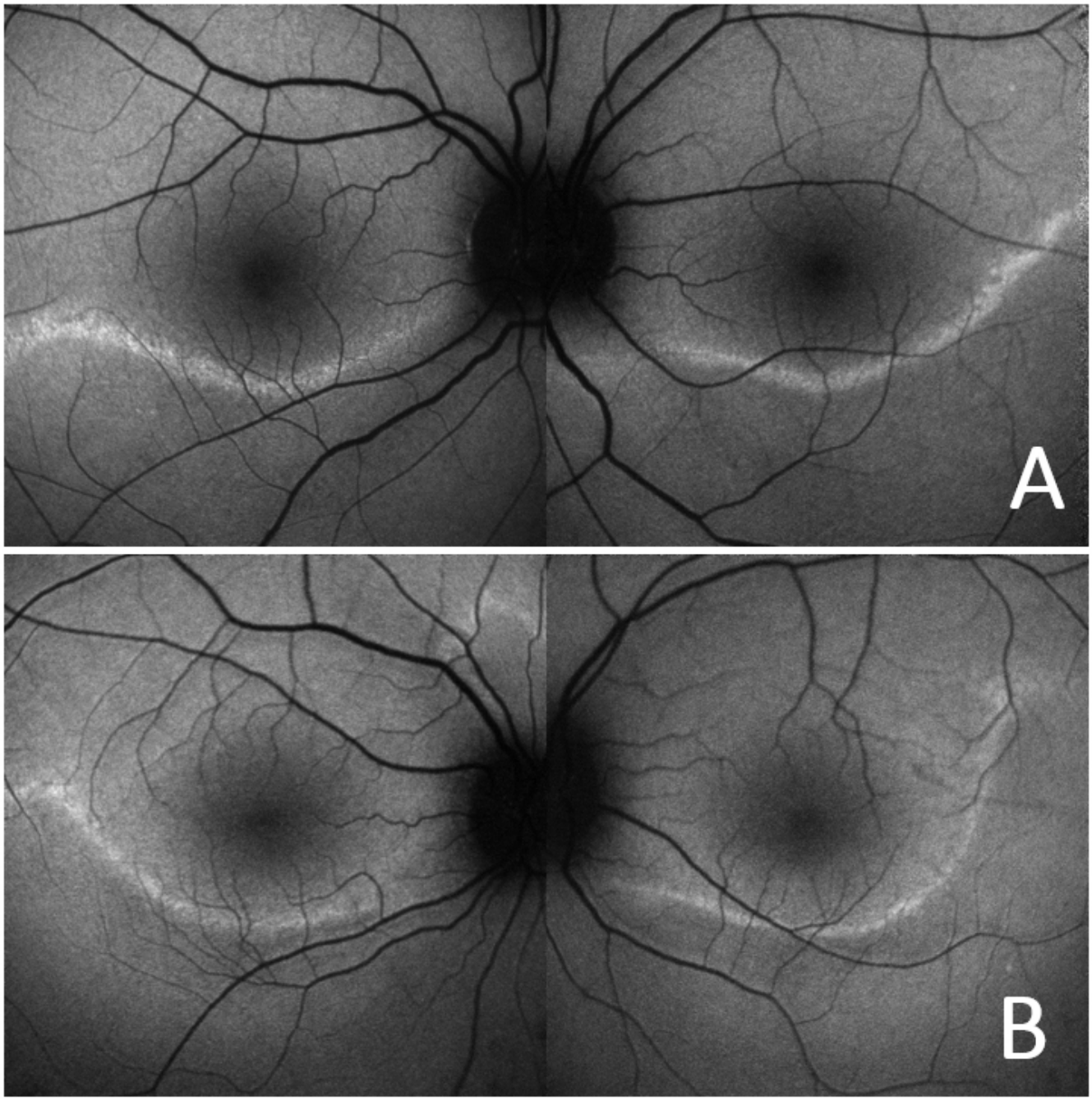

Figure 6. Fundus autofluorescence imaging. The images show the hyper-AF bands in the inferior sectors in patient 10 (**A**) and patient 11 (**B**). The continuous lines of higher autofluorescence outline the affected retina.

area seems to be similar to the transition zone described in classic RP with photoreceptor alterations but with an intact RPE with progression from periphery to the center [42-44].

Cystoid macular edema is often associated with classic RP with a prevalence of 10–15% [48]. However, in this cohort of patients with sector RP we found no evidence of macular edema on OCT; in two patients, we observed epiretinal membranes (ERM)s. The absence of macular edema represents an important finding in the clinical course of the disease. This could be related to lower inflammatory activation than that hypothesized for classic RP, given the topographic limitation of retinal alterations.

Visual field defects of varying extent have been reported in patients with sector RP [7-9,34-37]. For all the patients in the cohort, VF changes not only corresponded topographically to the retinal alterations (i.e., the superior scotoma corresponded to the dystrophic inferior retinal area) but also to the ophthalmoscopic abnormalities. This is in agreement with previous findings [7,9] excluding the one case reported by Coussa et al. [9] who showed ophthalmoscopic abnormalities in both eyes in the inferior retina associated with a concentric visual field constriction.

In addition, with regard to function, full-field ERG recordings showed varying degrees of impairment of rod function. There were no delays in implicit time but scotopic

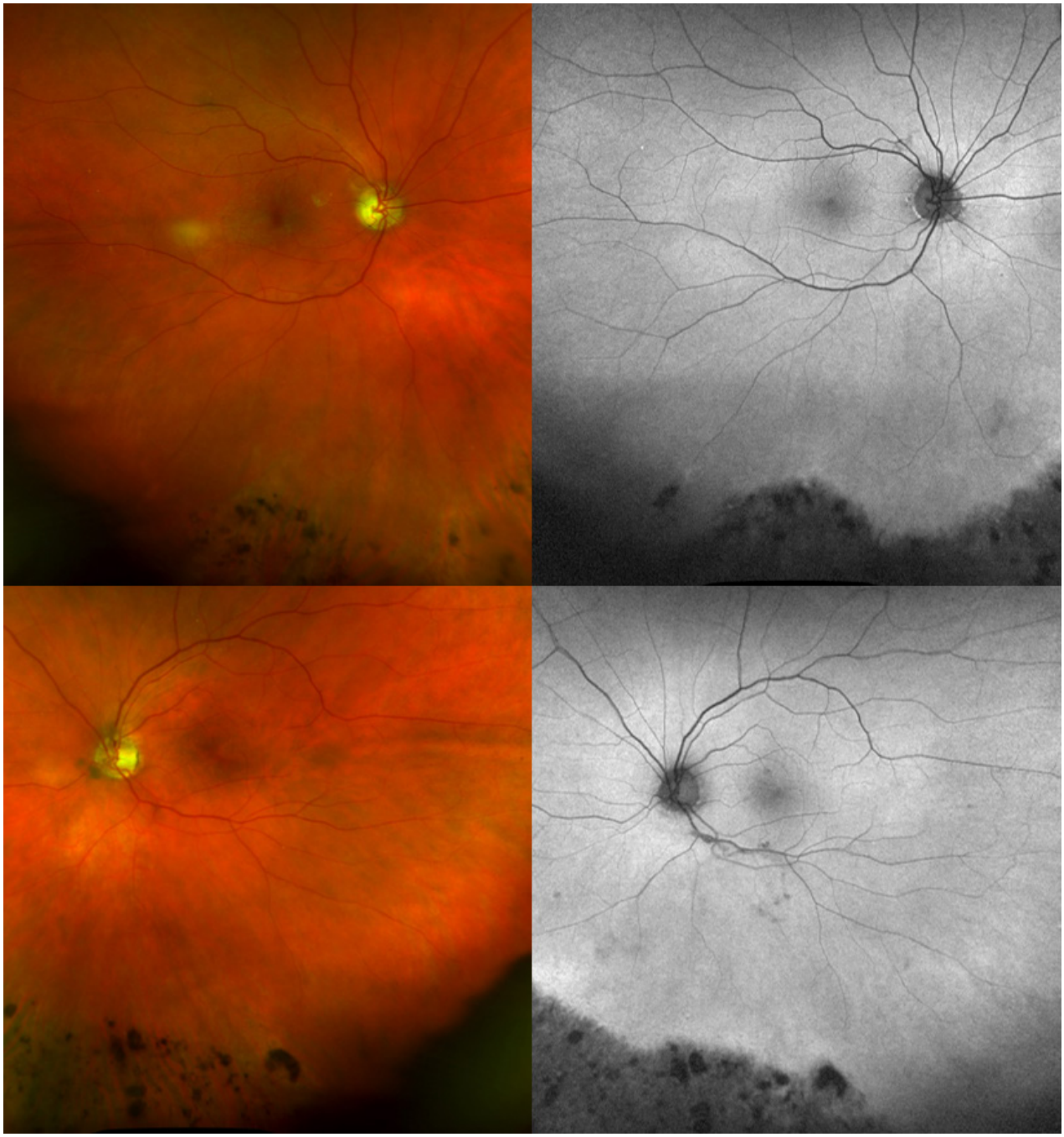

Figure 7. Widefield retinography and fundus autofluorescence imaging. The images show inferior pigmentary changes in the very periphery in patient 15.

ERG response amplitudes were decreased; however, they were less affected than in patients with classic RP [49]; the photopic ERG responses were within normal limits. Additional evidence that sector RP is characterized by limited retinal involvement and mild functional damage was provided in a recent study by Giambene et al. [38]. In that study, the cone-mediated multifocal ERG examination displayed significant differences between sector and generalized RP. The patients with sector RP had normal ERG amplitude and latency values even in pigmented areas.

The genetic analysis of the 11 screened patients showed pathogenic sequence variants in the *RHO* gene in

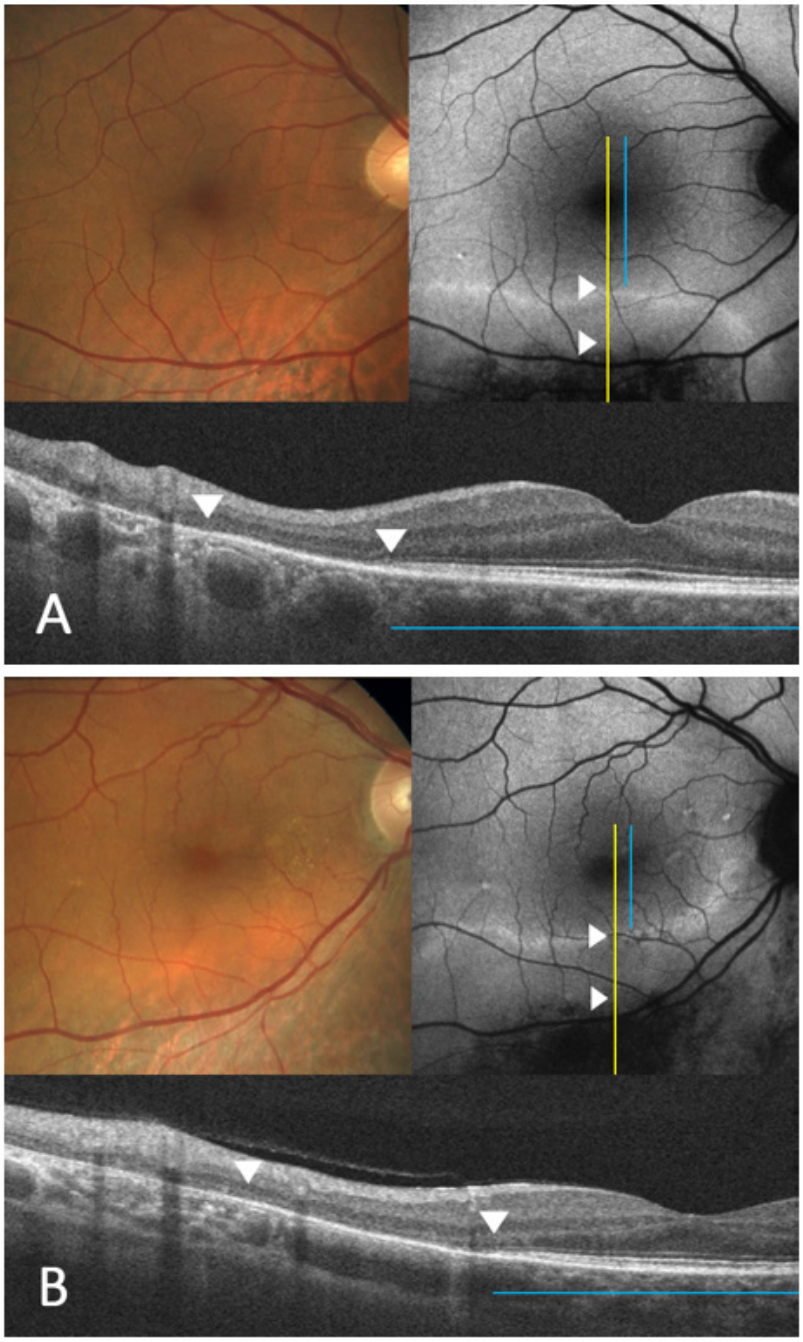

Figure 8. Fundus autofluorescence and OCT imaging. The images are referred to patient 2 (**A**) and patient 1 (**B**). The yellow line indicates the vertical OCT scan line passing through the hyper-AF demarcation line while the blue line indicates the intact EZ band. The two white arrows indicate the internal and external borders of the transition zone.

Table 2. Full-field ERG results in sector RP and a control group.

Variables	Sector RP (15)	Controls (15)	P value
Age	**50.14 +/−18.20**	**42.40 +/−10.78**	**0.15**
Dark adapted 0.01 ERG amplitude (μV)	33.78±13.17	121.50±22.91	<0.001
Dark adapted 3.0 ERG amplitude (μV)	117.84±24.24	141.81±23.05	<0.01
Light adapted 3.0 ERG amplitude (μV)	102.55±25.92	105.53±10.20	0.68
Dark adapted 0.01 ERG IT (msec)	75.49±15.46	75.19±7.81	0.95
Dark adapted 3.0 ERG IT (msec)	43.07±1.68	43.65±3.77	0.59
Light adapted 3.0 ERG IT (msec)	33.46±0.84	33.01±1.24	0.25

nine patients. Specifically, nine patients of four independent pedigrees carried the same *RHO* mutation c.568G>A p.(Asp190Asn), which has been reported in patients with retinitis pigmentosa [23-29]. Interestingly, most of the patients associated with this mutation presented with a classic RP phenotype. Park et al. [26] reported on a family in which the father and his younger son presented with a classic diffuse RP phenotype (even if the clinical picture was definitely more severe in the father), while the eldest son presented a sector RP phenotype with involvement of the inferior sector of the retina. Another case carried a different *RHO* sequence variant c.548T>C (p.Leu183Pro), but its interpretation with predictive software classified it as a VUS. These results are in agreement with those of other papers [7-14,50,51] reporting mutations in *RHO* in most of the patients affected by sector RP, even if the detected mutations are different from those of various ethnic groups. The data support the hypothesis that *RHO* sequence variants are the most commonly associated with the sector RP phenotype and suggest that priority should be given to the genetic analysis of the *RHO* gene during mutation screening of patients with sector RP. The detection of the same mutation in *RHO* c.568G>A p.(Asp190Asn) in the large majority of this genetically screened sector RP suggests that this variant could be peculiar to Italian patients with sector RP. The last screened patient can be considered genetically not characterized, as *USH2A* (Gene ID: 7399, OMIM

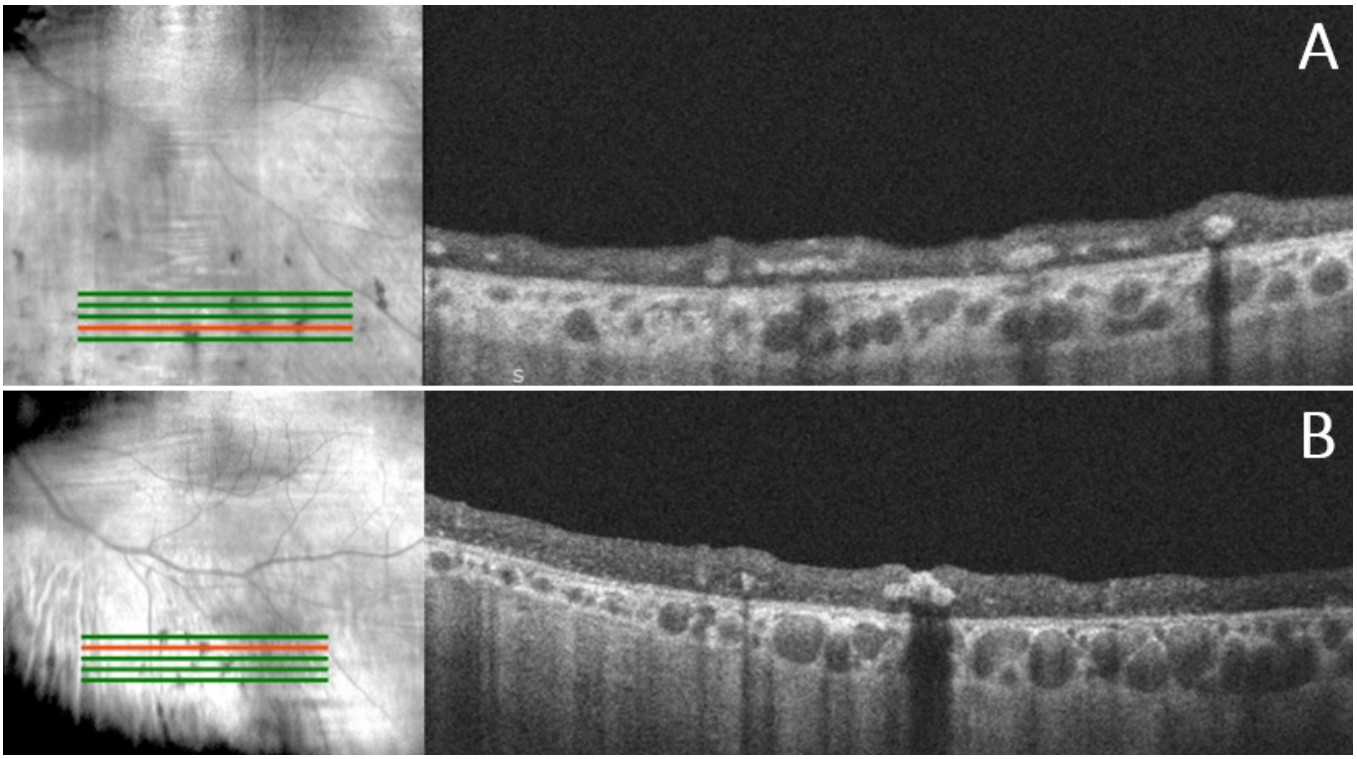

Figure 9. OCT scan at the level of bone spicules with an underlying choroid with prominent choroidal vessels.

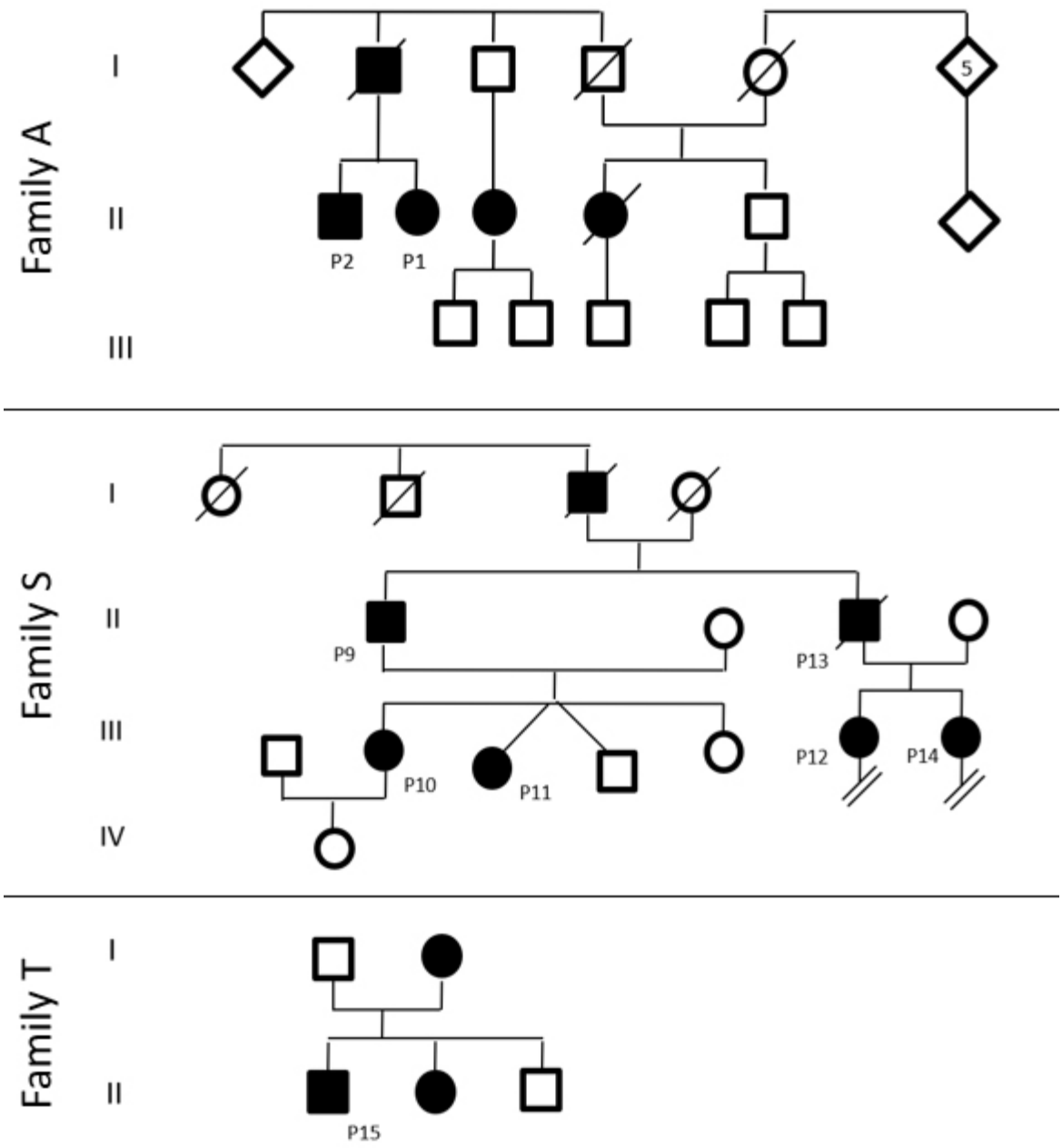

Figure 10. Autosomal dominant pedigrees of families A, S, and T.

608400) and *ROM1* (Gene ID: 6094, OMIM 180721) sequence variants are usually associated with recessive inheritance [31-33,52,53]. Nevertheless, in previous papers the same *ROM1* genotype c.178C>A (p.Pro60Thr) associated in "cis" with c.323C>T (p.Thr108Met) was hypothesized to be associated with an RP phenotype. This genotype was not definitely interpreted as pathogenic because of the small size of the pedigrees and the limited possibility of segregation analysis. Moreover, in this series the brother of the proband carries the same *ROM1* genotype (with the two variants in the same allele in "cis"), and he is still clinically healthy. Of course, we should consider the possibility of digenic inheritance mutations in *RHO* and *PRPH2* (Gene ID: 5961, OMIM 179605). In this patient, the NGS results did not show any alterations of the *PRPH2* gene, but as NGS can miss significant insertions and deletions, we could have also performed multiplex ligation-dependent probe amplification (MLPA) to exclude chromosomic rearrangements. Unfortunately, the patient

was not available for further molecular analysis. Thus, the pathogenicity of these *ROM1* variants remains questionable.

Of note, even if in this series *RHO* variants are the most common genetic determinants of sector RP (SRP), the report of a case not associated with mutations in *RHO* requires one to consider other possible genetic causes of sector RP phenotypes. This is in agreement with previous investigations reporting some sector RP cases that do not carry mutations in the *RHO* gene [7-9].

Similarly, with regard to clinical genetics, in this case series, three families presented more affected members with a clear dominant transmission. All other patients appeared to be sporadic, although it was difficult to classify them with accuracy given the impossibility of examining other family members. Sector RP is mostly associated with good visual acuity and limited changes in the visual field; thus, only a complete examination of the patient can allow one to exclude the disease. Therefore, at present no inheritance pattern can be completely excluded.

In families with more affected members (families A and S), we found in the series that the sector phenotype was transmitted from generation to generation. In all cases except one, the members of these families presented an alteration of the inferior retinal sector; only one patient presented a different alteration (nasal in one eye, temporal in the other). Therefore, this series, although limited, shows that it is possible to maintain a sector phenotype in successive generations. However, even if we did not have the chance to examine them directly, the cousin of patients P1 and P2 and the mother of patient P15 were reported to be classic RP phenotypes. This is in agreement with previous papers reporting a classic diffuse RP phenotype in the same patients carrying the *RHO* mutation c.568G>A p.(Asp190Asn) [24,25], while Park reported on a family in which this mutation is associated with a diffuse classic RP phenotype in the father and in the younger son but with a sector RP phenotype in the eldest son [26]. Finally, Xiao reported significant phenotypic variability and variable penetrance in his series of Chinese patients with sector RP [7]. These data strongly support a possible phenotypic variability in patients affected by sector RP.

The main limitations of this study are the small sample size with only a few evaluated families and the lack of longitudinal data. However, the analysis highlighted some important aspects of sector RP providing more information about the physiopathology of the disease and confirming, in the typical cases, the topographically limited involvement of the retinal degeneration process. Moreover, in this study we included only selected typical cases with clearly sectorial ophthalmoscopic and visual field abnormalities.

In conclusion, typical Italian patients with sector RP have normal visual acuity and generally a more favorable prognosis than other forms of RP. In most of the cases, the disease is associated with pathogenic mutations in the *RHO* gene with possible phenotypic variability even within the same family. Further investigations, including longitudinal studies with a long follow-up, are needed to clarify and define the natural history of the disease, to evaluate the possibility of unusual sector RP cases (i.e., disagreement between ophthalmoscopic retinal alterations and the extent of visual field loss) and to define the role of multimodal imaging for monitoring the progression of the disease for future therapeutic interventions. Moreover, even if *RHO* mutations are the most commonly reported in this series, the genotypic and phenotypic variability of sector RP is still to be fully determined.

ACKNOWLEDGMENTS

VG: Supported in part by grants from the National Eye Institute/NIH R01EY009076 and an unrestricted grant from the Research to Prevent Blindness to the Department of Ophthalmology, Columbia University. SHT: Conflict of interests: Scientific Advisory board member: Emendo. Supported by grants from the National Institute of Health 5P30CA013696, U01EY030580, U54OD020351, R24EY028758, R24EY027285, P30EY019007, R01EY018213, R01EY024698, R01EY026682, R21AG050437, the Schneeweiss Stem Cell Fund, New York State [SDHDOH01-C32590GG-3450000], the Foundation Fighting Blindness New York Regional Research Center Grant [PPA-1218–0751-COLU], Nancy & Kobi Karp, the Crowley Family Funds, The Rosenbaum Family Foundation, Alcon Research Institute, the Gebroe Family Foundation, the Research to Prevent Blindness (RPB) Physician-Scientist Award, and unrestricted funds from RPB, New York, NY, USA

REFERENCES

1. Bietti G. Su alcune forme atipiche o rare di degenerazione retinica (degenerazioni tapetoretiniche e quadri morbosi similari). Boll Ocul 1937; 16:1159-244. .

2. Krill AE, Archer D, Martin D. Sector retinitis pigmentosa. Am J Ophthalmol 1970; 69:977-87. [PMID: 5423778].

3. Grover S, Fishman GA, Alexander KR, Anderson RJ, Derlacki DJ. Visual acuity impairment in patients with retinitis pigmentosa. Ophthalmology 1996; 103:1593-600. [PMID: 8874431].

4. Farber MD, Fishman GA, Weiss RA. Autosomal dominantly inherited retinitis pigmentosa. Visual Acuity loss by subtype. Arch Ophthalmol 1985; 103:524-8. [PMID: 3985831].

5. Massof RW, Finkelstein D. Vision threshold profiles in sector retinitis pigmentosa. Arch Ophthalmol 1979; 97:1899-904. [PMID: 485914].

6. Hellner KA, Rickers J. Familiary bilateral segmental retinopathia pigmentosa. Ophthalmologica 1973; 166:327-41. [PMID: 4730724].

7. Xiao T, Xu K, Zhang X, Xie Y, Li Y. Sector Retinitis Pigmentosa caused by mutations of the RHO gene. Eye (Lond) 2019; 33:592-9. [PMID: 30390055].

8. Napier ML, Durga D, Wolsey CJ, Chamney S, Alexander S, Brennan R, Simpson DA, Silvestri G, Willoughby CE. Mutational Analysis of the Rhodopsin Gene in Sector Retinitis Pigmentosa. Ophthalmic Genet 2015; 36:239-43. [PMID: 25265376].

9. Coussa RG, Basali D, Maeda A, DeBenedictis M, Traboulsi EI. Sector retinitis pigmentosa: Report of ten cases and a review of the literature. Mol Vis 2019; 25:869-89. [PMID: 31908405].

10. Heckenlively JR, Rodriguez JA, Daiger SP. Autosomal dominant sectoral retinitis pigmentosa: two families with transversion mutation in codon 23 of rhodopsin. Arch Ophthalmol 1991; 109:84-91. [PMID: 1987955].

11. Sullivan LJ, Makris GS, Dickinson P, Mulhall LE, Forrest S, Cotton R, Loughnan MSA. New Codon 15 Rhodopsin Gene Mutation in Autosomal Dominant Retinitis Pigmentosa Is Associated With Sectorial Disease. Arch Ophthalmol 1993; 111:1512-7. [PMID: 8240107].

12. Rivera-De la Parra D, Cabral-Macias J, Matias-Florentino M, Rodriguez-Ruiz G, Robredo V, Zenteno JC. Rhodopsin p.N78I dominant mutation causing sectorial retinitis pigmentosa in a pedigree with intrafamilial clinical heterogeneity. Gene 2013; 519:173-6. [PMID: 23402891].

13. Shah SP, Wong F, Sharp DM, Vincent AL. A novel rhodopsin point mutation, proline-170-histidine, associated with sectoral retinitis pigmentosa. Ophthalmic Genet 2014; 35:241-7. [PMID: 24918165].

14. Ramon E, Cordomí A, Aguilà M, Srinivasan S, Dong X, Moore AT, Webster AR, Cheetham ME, Garriga P. Differential Light-Induced Responses in Sectorial Inherited Retinal Degeneration. J Biol Chem 2014; 26:35918-28. [PMID: 25359768].

15. Saihan Z, Stabej Ple Q, Robson AG, Rangesh N, Holder GE, Moore AT, Steel KP, Luxon LM, Bitner-Glindzicz M, Webster AR. Mutations in the USH1C gene 413 associated with sector retinitis pigmentosa and hearing loss. Retina 2011; 31:1708-414. [PMID: 21487335].

16. Branson SV, McClintic JI, Stamper TH, Haldeman-Englert CR, John VJ. Sector Retinitis Pigmentosa Associated with Novel Compound Heterozygous Mutations of CDH23. Ophthalmic Surg Lasers Imaging Retina 2016; 47:183-6. [PMID: 26878454].

17. Sato M, Oshika T, Kaji Y, Nose H. A novel homozygous Gly107Arg mutation in the RDH5 gene in a Japanese patient with fundus albipunctatus with sectorial retinitis pigmentosa. Ophthalmic Res 2004; 36:43-50. [PMID: 15007239].

18. Nakamachi Y, Nakamura M, Fujii S, Yamamoto M, Okubo K. Oguchi disease with sectoral retinitis pigmentosa harboring adenine deletion at position 1147 in the arrestin gene. Am J Ophthalmol 1998; 125:249-51. [PMID: 9467455].

19. Nguyen XT, Talib M, van Schooneveld MJ, Brinks J, Brink JT, Florijn RJ, Wijnholds J, Verdijk RM, Bergen AA, Boon CJF. RPGR-Associated Dystrophies: Clinical, Genetic, and Histopathological Features. Int J Mol Sci 2020; 21:835- [PMID: 32012938].

20. Chylack LT Jr, Wolfe JK, Singer DM, Leske MC, Bullimore MA, Bailey IL, Friend J, McCarthy D, Wu SY. The Lens Opacities Classification System III. The Longitudinal Study of Cataract Study Group. Arch Ophthalmol 1993; 111:831-6. [PMID: 8512486].

21. McCulloch DL, Marmor MF, Brigell MG, Hamilton R, Holder GE, Tzekov R, Bach M. ISCEV Standard for full-field clinical electroretinography (2015 update). Doc Ophthalmol 2015; 130:1-12. [PMID: 25502644].

22. Richards S, Aziz N, Bale S, Bick D, Das S, Gastier-Foster J, Grody WW, Hegde M, Lyon E, Spector E, Voelkerding K, Rehm H. ACMG Laboratory Quality Assurance Committee. Standards and guidelines for the interpretation of sequence variants: a joint consensus recommendation of the American College of Medical Genetics and Genomics and the Association for Molecular Pathology. Genet Med 2015; 17:405-24. [PMID: 25741868].

23. Keen TJ, Inglehearn CF, Lester DH, Bashir R, Jay M, Bird AC, Jay B, Bhattacharya SS. Autosomal dominant retinitis pigmentosa: four new mutations in rhodopsin, one of them in the retinal attachment site. Genomics 1991; 11:199-205. [PMID: 1765377].

24. Tsui I, Chou CL, Palmer N, Lin CS, Tsang SH. Phenotype-genotype correlations in autosomal dominant retinitis pigmentosa caused by RHO, D190N. Curr Eye Res 2008; 33:1014-22. [PMID: 19085385].

25. Kim C, Kim KJ, Bok J, Lee EJ, Kim DJ, Oh JH, Park SP, Shin JY, Lee JY, Gon Yu H. Microarray-based mutation detection and phenotypic characterization in Korean patients with retinitis pigmentosa. Mol Vis 2012; 18:2398-410. [PMID: 23049240].

26. Park SP, Lee W, Bae EJ, Greenstein V, Sin BH, Chang S, Tsang SH. Early Structural Anomalies Observed by High-Resolution Imaging in Two Related Cases of Autosomal-Dominant Retinitis Pigmentosa. Ophthalmic Surg Lasers Imaging Retina 2014; 45:469-73. [PMID: 25215869].

27. Jacobson SG, Cideciyan AV, Kemp CM, Sheffield VC, Stone EM. Photoreceptor function in heterozygotes with insertion or deletion mutations in the RDS gene. Invest Ophthalmol Vis Sci 1996; 37:1662-74. [PMID: 8675410].

28. Cideciyan AV, Hood DC, Huang Y, Banin E, Li ZY, Stone EM, Milam AH, Jacobson SG. Disease sequence from mutant rhodopsin allele to rod and cone photoreceptor degeneration

in man. Proc Natl Acad Sci USA 1998; 95:7103-8. [PMID: 9618546].

29. Jacobson SG, McGuigan DB 3rd, Sumaroka A, Roman AJ, Gruzensky ML, Sheplock R, Palma J, Schwartz SB, Aleman TS, Cideciyan AV. Complexity of the Class B Phenotype in Autosomal Dominant Retinitis Pigmentosa Due to Rhodopsin Mutations. Invest Ophthalmol Vis Sci 2016; 57:4847-58. [PMID: 27654411].

30. Costa KA, Salles MV, Whitebirch C, Chiang J, Juliana MFS. Gene panel sequencing in Brazilian patients with retinitis pigmentosa. Int J Retina Vitreous. 2017; 3:33-[PMID: 28912962].

31. Sakuma H, Inana G, Murakami A, Yajima T, Weleber RG, Murphey WH, Gass JD, Hotta Y, Hayakawa M, Fujiki K, Gao YQ, Dancinger M, Farber D, Cideciyan AV, Jacobson SJ. A heterozygous putative null mutation in ROM1 without a mutation in peripherin/RDS in a family with retinitis pigmentosa. Genomics 1995; 27:384-6. [PMID: 7558016].

32. Bascom RA, Liu L, Heckenlively JR, Stone EM, McInnes RR. Mutation analysis of the ROM1 gene in retinitis pigmentosa. Hum Mol Genet 1995; 4:1895-902. [PMID: 8595413].

33. Martinez-Mir A, Vilela C, Bayes M, Valverde D, Dain L, Beneyto M, Marco M, Baiget M, Grinberg D, Balcells S, Gonzalez-Duarte R, Vilageliu L. Putative association of a mutant ROM1 allele with retinitis pigmentosa. Hum Genet 1997; 99:827-30. [PMID: 9187681].

34. Meyerle CB, Fisher YL, Spaide RF. Autofluorescence and visual field loss in sector retinitis pigmentosa. Retina 2006; 26:248-50. [PMID: 16467695].

35. Fleckenstein M, Charbel Issa P, Fuchs HA, Finger RP, Helb HM, Scholl HPN, Holz FG. Discrete arcs of increased fundus autofluorescence in retinal dystrophies and functional correlate on microperimetry. Eye (Lond) 2009; 23:567-75. [PMID: 18344954].

36. Balikoglu-Ylmaz M, Taskapili M, Yilmaz T, Teke MY. Optic disc pit with sectorial retinitis pigmentosa. Case Rep Ophthalmol Med 2013; •••:156023-[PMID: 23781365].

37. Robson AG, Saihan Z, Jenkins SA. Functional characterization and serial imaging of abnormal fundus autofluorescence in patients with retinitis pigmentosa and normal visual acuity. Br J Ophthalmol 2006; 90:472-9. [PMID: 16547330].

38. Giambene B, Verdina T, Pennino M, Fabbrucci M, Cavallini GM, Menchini U. Multifocal electroretinographic responses in sector retinitis pigmentosa. Int Ophthalmol 2020; 40:703-8. [PMID: 31758507].

39. Hartong DT, Berson EL, Dryja TP. Retinitis pigmentosa. Lancet 2006; 18:1795-809. [PMID: 17113430].

40. McDonald HR, Schatz H, Johnson RN. Ocular phototoxicity. Curr Opin Ophthalmol 1990; 1:280-4. .

41. Schwartz L, Boëlle PY, D'hermies F, Ledanois G, Virmont J. Blue light dose distribution and retinitis pigmentosa visual field defects: an hypothesis. Med Hypotheses 2003; 60:644-9. [PMID: 12710896].

42. Popovic P, Jarc-Vidmar M, Hawlina M. Abnormal fundus autofluorescence in relation to retinal function in patients with retinitis pigmentosa. Graefes Arch Clin Exp Ophthalmol 2005; 243:1018-27. [PMID: 15906064].

43. Fleckenstein M, Charbel Issa P, Helb HM, Schmitz-Valckenberg S, Scholl HP, Holz FG. Correlation of lines of increased autofluorescence in macular dystrophy and pigmented paravenous retinochoroidal atrophy by optical coherence tomography. Arch Ophthalmol 2008; 126:1461-3. [PMID: 18852430].

44. Lima LH, Cella W, Greenstein VC, Wang NK, Busuioc M, Smith RT, Yannuzzi LA, Tsang SH. Structural assessment of hyperautofluorescent ring in patients with retinitis pigmentosa. Retina 2009; 29:1025-31. [PMID: 19584660].

45. Wakabayashi T, Sawa M, Gomi F, Tsujikawa M. Correlation of fundus autofluorescence with photoreceptor morphology and functional changes in eyes with retinitis pigmentosa. Acta Ophthalmol 2010; 88:177-83. [PMID: 20491687].

46. Murakami T, Akimoto M, Ooto S, Suzuki T, Ikeda H, Kawagoe N, Takahashi M, Yoshimura N. Association between abnormal autofluorescence and photoreceptor disorganization in retinitis pigmentosa. Am J Ophthalmol 2008; 145:687-94. [PMID: 18242574].

47. Duncker T, Lee W, Tsang SH, Greenberg JP, Zernant J, Allikmets R, Sparrow JR. Distinct characteristics of inferonasal fundus autofluorescence patterns in stargardt disease and retinitis pigmentosa. Invest Ophthalmol Vis Sci 2013; 54:6820-6. [PMID: 24071957].

48. Scorolli L, Morara M, Meduri A, Reggiani LB, Ferreri G, Scalinci SZ, Meduri RA. Treatment of cystoid macular edema in retinitis pigmentosa with intravitreal triamcinolone. Arch Ophthalmol 2007; 125:759-64. [PMID: 17562986].

49. Berson EL. Electroretinographic findings in retinitis pigmentosa. Jpn J Ophthalmol 1987; 31:327-48. [PMID: 2448510].

50. Wanga J, Xua D, Zhub T, Zhoub Y, Chenb X, Wanga F, Zhanga J, Tiana H, Gaoa F, Zhanga J, Jina C, Xua J, Lua L, Liuc Q, Xua GT. Identification of two novel RHO mutations in Chinese retinitis pigmentosa patients. Exp Eye Res 2019; 188:107726-[PMID: 31319082].

51. Katagiri S, Hayashi T, Akahori M, Itabashi T, Nishino J, Yoshitake K, Furuno M, Ikeo K, Okada T, Tsuneoka H, Iwata T. RHO Mutations (p.W126L and p.A346P) in Two Japanese Families with Autosomal Dominant Retinitis Pigmentosa. J Ophthalmol 2014; 2014:210947-[PMID: 25485142].

52. Rivolta C, Berson EL, Dryja TP. Paternal uniparental heterodisomy with partial isodisomy of chromosome 1 in a patient with retinitis pigmentosa without hearing loss and a missense mutation in the Usher syndrome type II gene USH2A. Arch Ophthalmol 2002; 120:1566-71. [PMID: 12427073].

53. Aller E, Jaijo T, Beneyto M, Nájera C, Oltra S, Ayuso C, Baiget M, Carballo M, Antiñolo G, Valverde D, Moreno F, Vilela C, Collado D, Pérez-Garrigues H, Navea A, Millán JM. Identification of 14 novel mutations in the long isoform of USH2A in Spanish patients with Usher syndrome type II. J Med Genet 2006; 43:e55-[PMID: 17085681].

Articles are provided courtesy of Emory University and the Zhongshan Ophthalmic Center, Sun Yat-sen University, P.R. China. The print version of this article was created on 5 February 2021. This reflects all typographical corrections and errata to the article through that date. Details of any changes may be found in the online version of the article.